2022
9(2), 125-131

Journal of
MATERIALS NANOSCIENCE

Delta arsenene nanoribbon as a sensing element towards phenol and benzene vapours – a first- principles insight

V. Nagarajan, R. Chandiramouli*

School of Electrical & Electronics Engineering SASTRA Deemed University, Tirumalaisamudram, Thanjavur -613 401, India

Submitted on: 29-Oct-2021, Accepted and Published on: 15-Feb-2022

Research Article

ABSTRACT The advancement in nanomaterials opens the gate for various sensing substrates towards gas/vapours. In the current work, delta arsenene nanoribbon (δ-AsNR) is used as adsorbing element towards phenol and benzene vapours. The formation energy of δ-AsNR is recorded as -4.117 eV/atom confirming the stable structural geometry. The band gap of bare δ-AsNR is calculated to be 1.368 eV in the GGA/B86LYP level of theory. Furthermore, the adsorption of phenol and benzene vapours on δ-AsNR exhibits physisorption with the exothermic nature of adsorption. The charge transfer reveals that phenol and benzene molecules resemble donors and δ-AsNR as the acceptor of electrons. Besides, the projected density of states and band structure variation is noticed owing to the adsorption of phenol and benzene molecules on δ -AsNR. Hence, it is evident that δ -AsNR is one of the base substrates to sense the presence of phenol and benzene vapours in the environment.

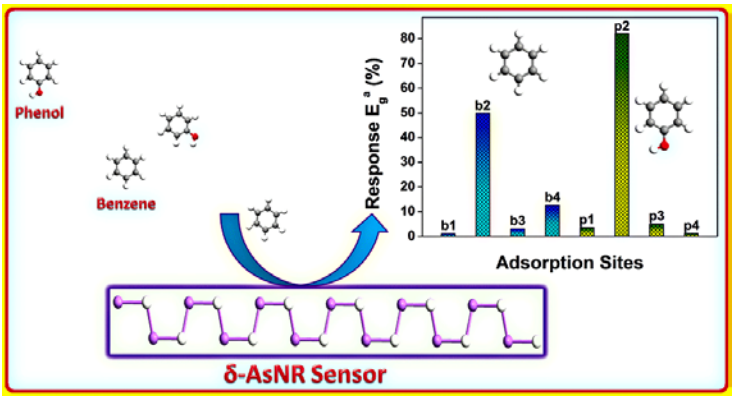

Keywords: Arsenene, Nanoribbon, Physisorption, Benzene, Phenol

INTRODUCTION

The advancement of two-dimensional (2D) material graphene opens the gate for other layered 2D materials. The sp^2 hybridized graphene suffers 0 eV, which makes it unsuitable for various applications. Thus, there is a search among the researchers for other 2D materials such as germanene, silicene, phosphorene, antimonene, arsenene etc.[1-5] The recent technological advancement leads to the exfoliation of layers from arsenic, which leads to the synthesis of arsenene.[6,7] The electronic properties of arsenene can be tailored with doping, functionalisation, and edge border effects. Moreover, different form factors of nanostructures can be obtained in arsenene, such as nanosheet, nanoribbon, and nanotubes. Zhi Zeng group[8] reported spin density waves observed in zigzag arsenene, antimonene, and phosphorene. The spin density wave can be fine-tuned by doping and strains. Y. R. Wang et al.[9] observed indirect to direct band gap transition owing to doping of P, Sb, and Bi in puckered arsenene. Kai-Wei Yang et al.[10] studied the transport properties of armchair arsenene nanoribbons with regard to the spin mechanism. Using the first-principles study, the energetics, magnetic, and electronic properties of Si, F, B, N, O, S, C, P, and H doped arsenene sheets are studied by Yu Yan group.[11] The study reveals that doping C, Si, O, and S on arsenene sheets exhibit a magnetic moment of 1.0 μ_B. The optical properties of monolayer buckled and washboard arsenene and bilayers are investigated by S. Ciraci et al.[12] The in-plane tensile strain, number of layers show the effect on the optical properties of 2D arsenene.

Benzene is a constituent of crude oil and a major industrial chemical. It finds its applications in the manufacturing of plastics, polymers, detergents, dyes, drugs, pesticides, and explosives. In spite of its wide applications, exposure to benzene vapours leads to lung, kidney, heart, liver, and brain problems. Benzene is also highly carcinogenic and causes myeloid leukemia, aplastic anemia.[13] Phenol is a good disinfectant, antiseptic drug, used in the production of phenolic resins, synthetic fibers, plasticizers, solvents, paints & coatings, and nylon. The Permissible Exposure Limit based on OSHA Standard for phenol is 5 ppm. The adverse effects of phenol include irritation to the eyes, skins, mucous membranes, diarrhea, vertigo, and salivation.[14] The metal oxide-based sensors are used to detect the presence of phenol and benzene.[15,16] Usually, metal

*Corresponding Author: Dr. R. Chandiramouli, School of Electrical & Electronics Engineering, SASTRA Deemed University, Thanjavur.
Tel: +919489566466
E-mail: rcmoulii@gmail.com

URN:NBN:sciencein.jmns.2022.v9.284

ISSN: 2394-0867
https://pubs.thesciencein.org/jmns

oxide-based sensors require high operating temperatures and lack selectivity. Nowadays, elemental monolayer-based chemical sensors are emerging as an alternative to metal oxide sensors. In the proposed work, we studied the sensing response of delta arsenene nanoribbon (δ-AsNR) as a sensing medium towards phenol and benzene and the results are discussed.

COMPUTATIONAL SPECIFICATION

Using QuantumATK - Atomistic Simulation Software, the structural stability and electronic properties of δ-AsNR are calculated.[17] We used the GGA/B86LYP level of theory for studying the adsorption properties of phenol and benzene on δ-AsNR.[18,19] Since the proposed work involves the adsorption of phenol and benzene on δ-AsNR, Grimme's DFT-D3 correction is used in the proposed study.[20] In order to carry out the structural optimisation of δ-AsNR, the grid mesh cut-off is held at 500 eV. The Hellmann-Feynman force of 0.02 eV/Å was utilised along with the conjugate gradient procedure. We employed double zeta polarisation basis set with 16 Å vacuum spacing between the adjacent layers to remove the field effects of adjacent layers.[21,22] Besides, the Monkhorst–Pack grid of $1 \times 1 \times 18$ is employed for Brillouin zone sampling. The energy convergence between the adjacent iteration is kept at 10^{-6} eV.

RESULTS AND OUTCOME

Structural and electronic properties of δ-AsNR

δ-AsNR belong to Pbcm (No. 57) space group with the lattice constants of δ-AsNR is calculated as $a = 5.90$ Å $and\ b = 5.88$ Å.[23] The bond distance and thickness of δ-AsNR are found to be 2.49 Å and 2.39 Å, respectively. To get the finite base material, δ-AsNR is passivated with the hydrogen atom at the terminating end which leads to an increase in the band gap. Figure 1 illustrates the structure of δ-AsNR. δ-AsNR is extended along the z-direction and the edges are passivated with hydrogen atoms to eradicate the adsorption of target phenol and benzene along the edges of δ-AsNR.

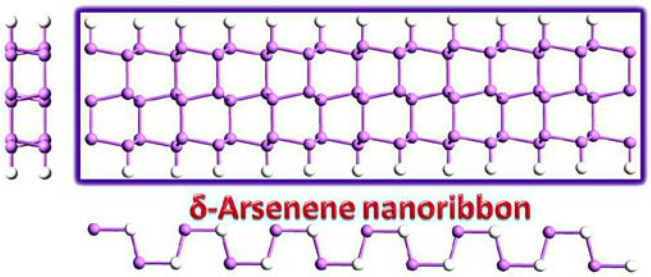

Figure 1 Schematic diagram of pristine δ-AsNR

Now the stability of δ-AsNR is to be ascertained based on the formation energy E_{fe} given by the expression below.[24,25]

$$E_{fe} = (1/r)[E(\delta\text{-AsNR}) - xE(As) - yE(H)]$$

Where $E(\delta - AsNR)$ denotes the energy of bare δ-AsNR, 'r' denotes the count of arsenic and hydrogen atoms, x and y represent the number of arsenic and hydrogen atoms, respectively, $E(As)$is the energy of the isolated arsenic atom and $E(H)$ is the energy of isolated hydrogen atom. The calculated value of E_{fe} is recorded as - 4.117 eV per atom. The negative value of δ-AsNR ensures the stable structure of δ-AsNR. The band structure and partial density of states (PDOS) provide insights into the nature of the base material δ-AsNR.[26-31] Figure 2 signifies the PDOS map and band structure of bare δ-AsNR. The band structure of δ-AsNR points out the semiconductor nature with the energy band gap of 1.368 eV inferred from the gamma point. Also, the band gap of δ-AsNR is tunable with ribbon width, edge bordering effects, and dopants. The sensing response of delta arsenene nanoribbon can be fine-tuned based on these factors. The PDOS map shows the peaks at -0.9 eV, -1.4 eV, and -1.8 eV in the valence band. Besides, in the conduction band peaks are observed at 0.75 eV, 1.5 to 1.8 eV. Also, the contribution of *p*-orbital of arsenic is dominant to the total DOS confirmed from the PDOS map.

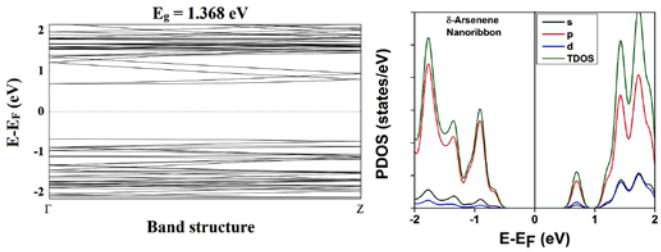

Figure 2 Band structure and PDOS spectrum of δ-AsNR

Benzene and Phenol adsorption studies on delta AsNR

Before studying the adsorption of benzene and phenol, we considered all possible adsorption configurations, and only for the discussed orientations, we obtained the minimum energy or global minima positions. Figure 3 a-d depicts the adsorption of benzene molecules on bridge site, parallel site, top site, and valley site, which are named as position b1, b2, b3, and b4, respectively. In a similar way, the adsorption of phenol molecules on the bridge site, parallel site, top site, and valley site of δ-AsNR are called as positions p1, p2, p3, and p4 correspondingly as presented in Figure 3 e-h.

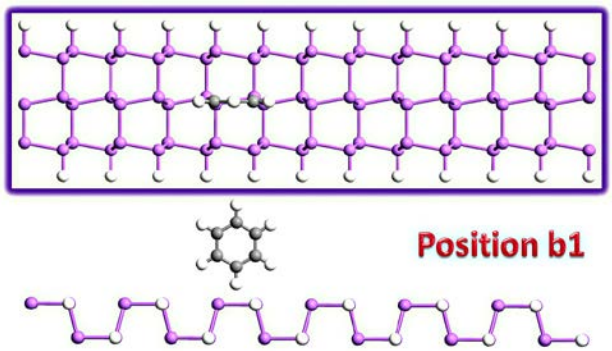

Figure 3 (a) Adsorption of benzene on bridge site of δ-AsNR – position b1

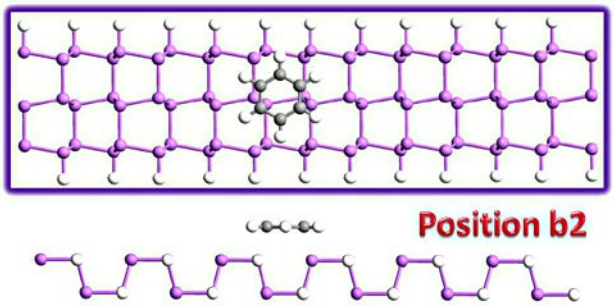

Figure 3 (b) Adsorption of benzene on parallel site of δ-AsNR – position b2

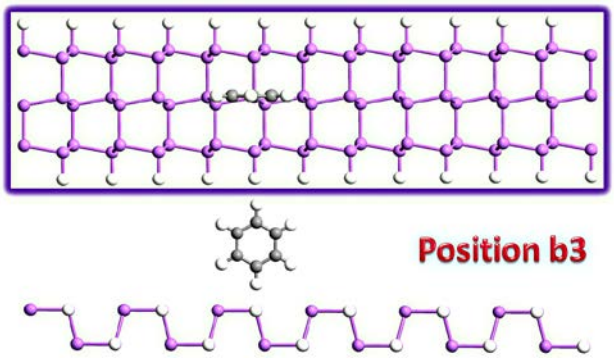

Figure 3 (c) Adsorption of benzene on top site of δ-AsNR – position b3

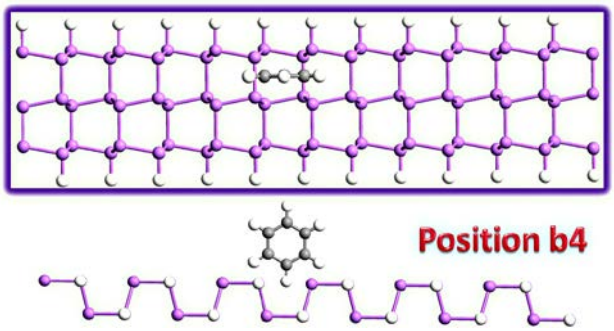

Figure 3 (d) Adsorption of benzene on valley site of δ-AsNR – position b4

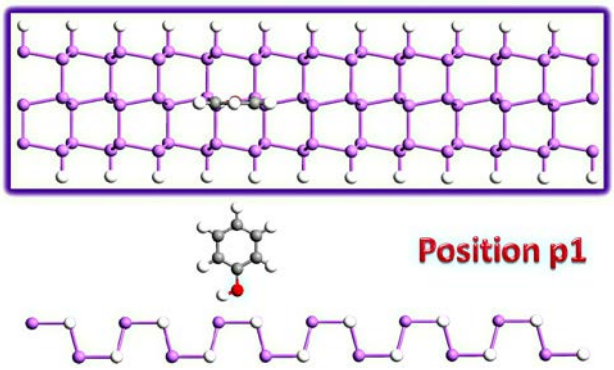

Figure 3 (e) Adsorption of phenol on bridge site of δ-AsNR – position p1

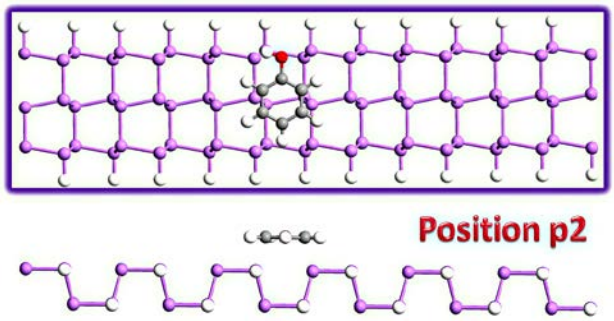

Figure 3 (f) Adsorption of phenol on parallel site of δ-AsNR – position p2

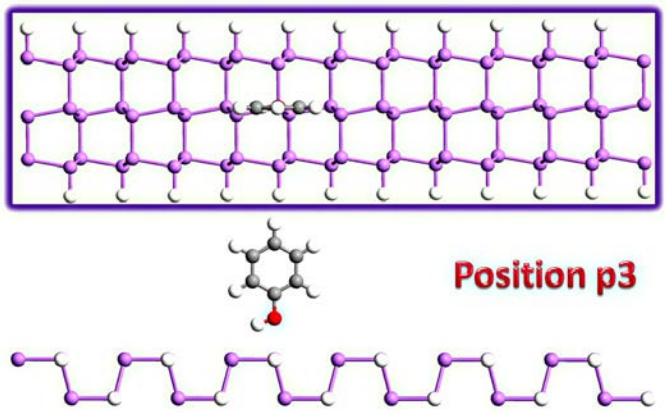

Figure 3 (g) Adsorption of phenol on top site of δ-AsNR – position p3

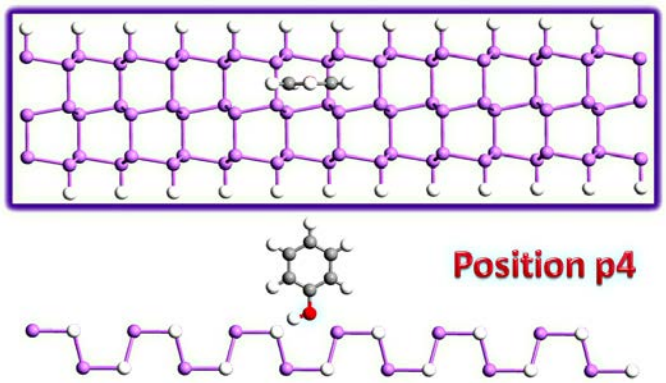

Figure 3 (h) Adsorption of phenol on valley site of δ-AsNR – position p4

The adsorption energy E_a plays a crucial role to decide the adsorption nature of target benzene and phenol molecules on δ-AsNR.[32-37]. The adsorption energy is calculated as given below

$$E_a = [E(\text{complex}) - E(\delta - \text{AsNR}) - E(benzene\ or\ phenol) + E(BSSE)]$$

where $E(\text{complex})$ is the energy of δ-AsNR with adsorbed benzene or phenol molecules, $E(\delta - \text{AsNR})$is the energy of isolated δ-AsNR, $E(benzene\ or\ phenol)$ is the energy of bare benzene or phenol molecule and $E(BSSE)$ is the basis set superposition error for removing the overlapping effects of basis set. Table. 1 presents the adsorption energy, band gap, average

band gap variation, and charge transfer owing to benzene and phenol adsorption on δ-AsNR. Moreover, E_a is recorded as -0.221, -0.415, -0.109, and -0.643 eV for positions b1, b2, b3 and b4 correspondingly. The phenol adsorption logs the value of -0.121, -0.639, -0.083 and -0.254 eV for positions p1, p2, p3 and p4, respectively. The negative value of E_a supports the exothermic adsorption of benzene and phenol vapours on δ-AsNR. Also, the E_a values infer that physical adsorption takes place owing to benzene and phenol adsorption on δ-AsNR. From the E_a results, it is evident that δ-AsNR is a suitable substrate for the detection of benzene and phenol vapours. The charge transfer (Q) throws the light on the donor/acceptor nature of δ-AsNR due to benzene and phenol adsorption.[38-41] Further to add, it is known that the value of Q possesses a positive magnitude, which infers that benzene and phenol molecules donate the electrons to δ-AsNR. Thus, the change in electronic properties occurs due to the adsorption of benzene and phenol effectuated due to charge transfer.

Table 1 Adsorption energy (E_a),Bader charge transfer (Q), energy gap (E_g)and average band gap variation (E_g^a) of chief molecules adsorbed δ-AsNR

$\boldsymbol{Nanostructure}$	$\boldsymbol{E_a\ (eV)}$	$\boldsymbol{Q\ (e)}$	$\boldsymbol{E_g\ (eV)}$	$\boldsymbol{E_g^a}$ (%)
$\delta - AsNR$	–	–	1.368	–
$Position\ b1$	-0.221	0.118	1.353	1.10
$Position\ b2$	-0.415	0.059	0.686	49.85
$Position\ b3$	-0.109	0.144	1.326	3.07
$Position\ b4$	-0.643	0.104	1.196	12.57
$Position\ p1$	-0.121	0.068	1.318	3.65
$Position\ p1$	-0.639	0.021	0.245	82.09
$Position\ p3$	-0.083	0.006	1.299	5.04
$Position\ p4$	-0.254	0.081	1.351	1.24
Other interfering gases				
$\delta - AsNR - CO$	-0.147	-0.048	1.333	2.56
$\delta - AsNR - CO_2$	-0.180	-0.121	1.344	1.75
$\delta - AsNR - H_2O$	-0.180	-0.121	1.339	2.12

The average energy band gap variation E_g^a confirms the electroresistive nature of δ-AsNR upon benzene and phenol adsorption.[42-45] Upon adsorption of benzene for positions it is observed that for positions b1, b2, b3, and b4, E_g^a variations are found to be 1.1, 49.85, 3.07, and 12.57% respectively. However, the phenol adsorption changes E_g^a to 3.65, 82.09, 5.04, and 1.24% for positions p1, p2, p3, and p4 correspondingly. Thus, it is inferred that the adsorption of benzene and phenol changes the resistive nature of δ-AsNR.

The changes in the electronic attributes of δ-AsNR are inferred from the band structure and PDOS map results.[46-50] Figure 4a-d illustrates the PDOS map and band structure diagram of δ-AsNR upon benzene adsorption. Likewise, Figure 4e-h depicts the changes in the band structure and PDOS map due to phenol adsorption. Moreover, due to benzene adsorption, it is clear that the peak positions changes for positions b1, b2, b3, and b4 compared to the PDOS spectrum of bare δ-AsNR. Also, the phenol adsorption follows the same trend in the peak shift for global minima positions p1, p2, p3, and p4 correspondingly. From the band structure and PDOS maps, the band gap of 1.353, 0.686, 1.326, and 1.196 eV is observed for positions b1, b2, b3, and b4, respectively. Besides, the band gap change of 1.318, 0.245, 1.299, and 1.351 eV is noticed for positions p1, p2, p3, and p4. Also from the PDOS maps, it exposed that the share of *p*-orbital is predominant towards the total density of states.

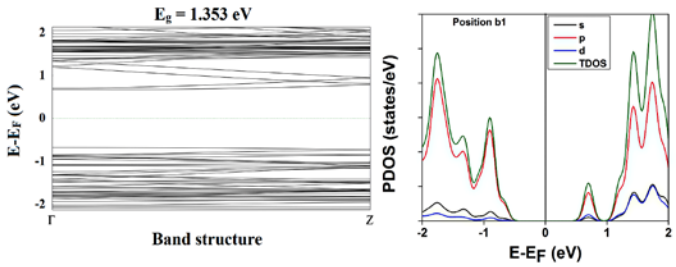

Figure 4 (a) Band structure and PDOS spectrum – position b1

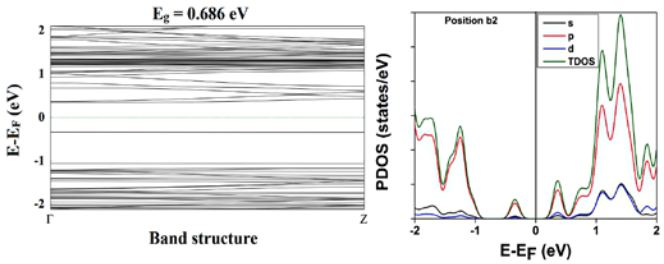

Figure 4 (b) Band structure and PDOS spectrum – position b2

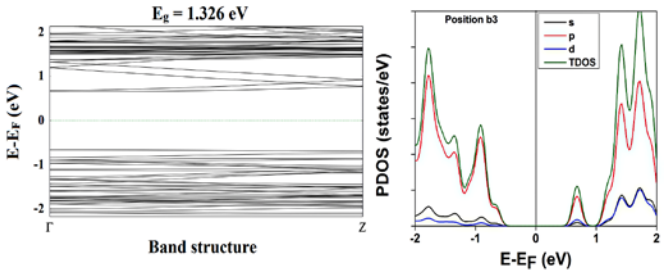

Figure 4 (c) Band structure and PDOS spectrum – position b3

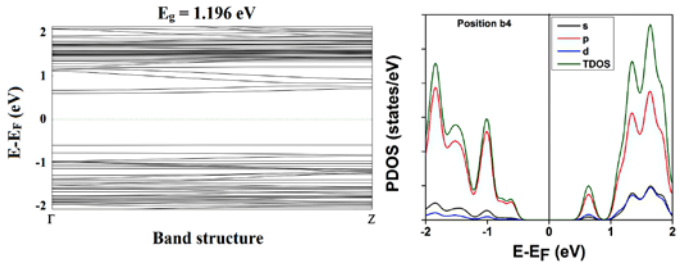

Figure 4 (d) Band structure and PDOS spectrum – position b4

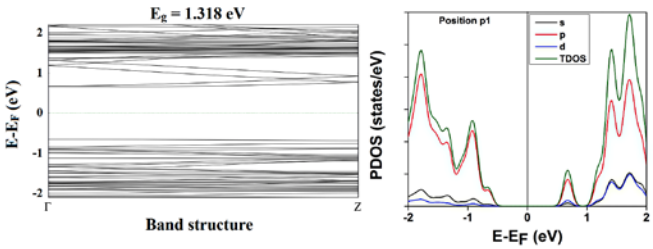

Figure 4 (e) Band structure and PDOS spectrum – position p1

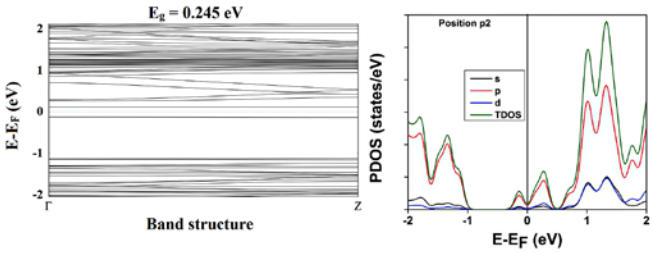

Figure 4 (f) Band structure and PDOS spectrum – position p2

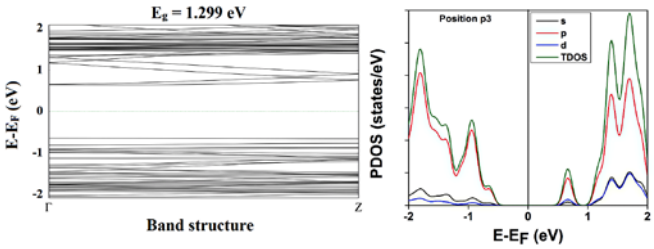

Figure 4 (g) Band structure and PDOS spectrum – position p3

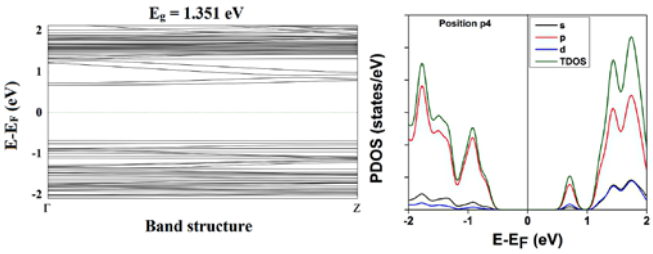

Figure 4 (h) Band structure and PDOS spectrum – position p4

The electron density map inputs the variations in the charge density owing to benzene and phenol adsorption on δ-AsNR [51-55]. Figure 5 presents the electron difference density of δ-AsNR in isolated conditions. Figure 6 a and b picture the electron difference density upon benzene and phenol adsorption on δ-AsNR. The deviations in the electron density are perceived in spite of benzene and phenol adsorption on δ-AsNR. Moreover, the benzene and phenol act as a donor of electrons, which is noticed by the blue colour gradient over benzene and phenol molecules. However, the base substrate δ-AsNR behaves as an acceptor of electron indicated with the red colour gradient over δ-AsNR. Hence, it is evident from the electron density difference, band structure, and PDOS spectrum that the changes in the electronic properties occur upon benzene and phenol adsorption on δ-AsNR.

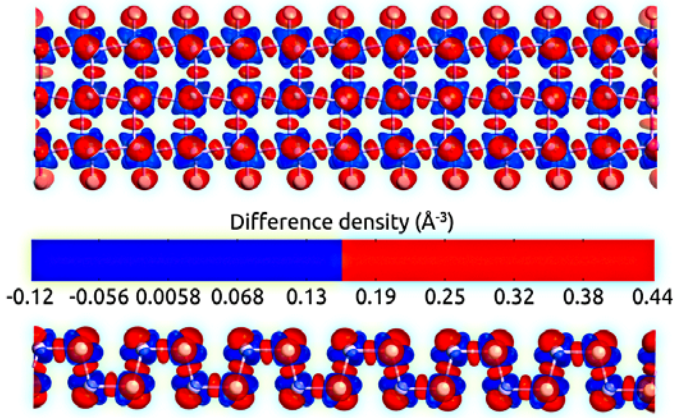

Figure 5 Electron difference density of isolated δ-AsNR

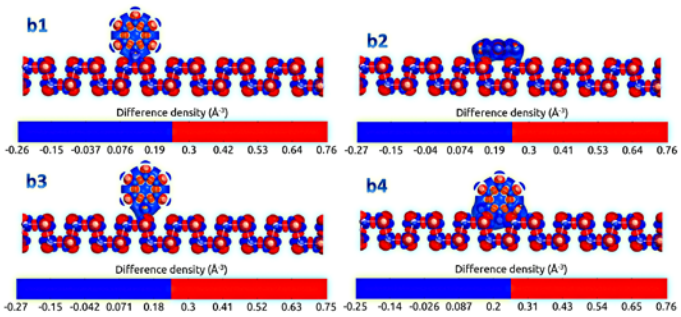

Figure 6 (a) Electron difference density – position b1,b2, b3 & b4

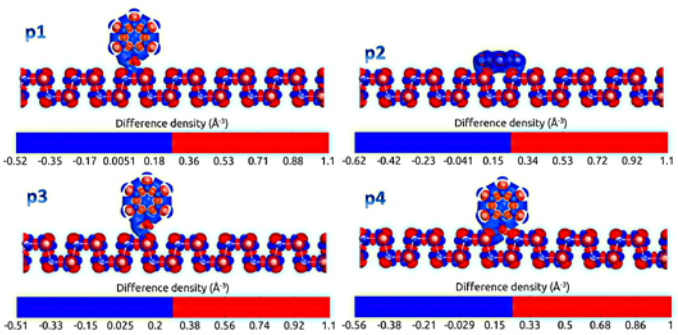

Figure 6 (b) Electron difference density – position p1, p2, p3 & p4

In order to verify the selectivity of δ-AsNR to chief molecules i.e. benzene and phenol in the air environment, we have also explored the sensing behaviour of other expected interfering gas molecules namely CO, CO_2, and H_2O (humidity). Figure S1 (see the supplementary information) refers to the band structure of δ-AsNR after interacting with CO, CO_2, and H_2O molecules, correspondingly. As a result, it is confirmed that the variation of band gap of δ-AsNR upon the adsorption of interfering gases is relatively lower than target molecules (benzene and phenol). Based on the overall result, it can be recommended that the δ-AsNR can be practically used as a chemical sensor to detect benzene and phenol in the air atmosphere.

CLOSING REMARKS

In the framework of the DFT method, the structural stability of δ-AsNR is explored in terms of formation energy and found to be stable. Hence, δ-AsNR is used as adsorbing substrates for benzene and phenol vapours. The changes in the electronic properties are noticed with reference to electron density difference, PDOS map, and band structure diagram. The variation in the band gap is observed owing to benzene and phenol adsorption. Moreover, benzene and phenol adsorption on δ-AsNR indicates physical adsorption revealed by adsorption energy. Besides, the charge transfer also occurs and target benzene and phenol molecules behave as the donor of electrons. The E_g^a study infers the electroresistive nature of δ-AsNR, which supports that δ-AsNR can be used as a two-electrode system to detect the presence of benzene and phenol in the vicinity.

CONFLICTS OF INTEREST

The authors declare that there are no conflicts of interest with respect to the research, authorship, and/or publication of this article.

ACKNOWLEDGEMENT

The authors wish to express their sincere thanks to Nano Mission Council, Department of Science & Technology, India (No.SR/NM/NS-1011/2017(G)) for the financial support

REFERENCES

1. F. Ersan, D. Kecik, V.O. Özçelik, Y. Kadioglu, O.Ü. Aktürk, E. Durgun, E. Aktürk, S. Ciraci. Two-dimensional pnictogens: A review of recent progresses and future research directions. *Applied Physics Reviews* **2019**, 6, 021308.
2. S. Zhang, M. Xie, F. Li, Z. Yan, Y. Li, E. Kan, W. Liu, Z. Chen, H. Zeng. Semiconducting Group 15 Monolayers: A Broad Range of Band Gaps and High Carrier Mobilities. *Angew. Chem. Int. Ed.* **2015**, 55, 1666–1669.
3. W. Yang, Q. Lyu, J. Zhao, L. Cao, Y. Hao, H. Zhang. Recent advance in near-infrared/ultrasound-sensitive 2D-nanomaterials for cancer therapeutics. *Sci. China Mater.* **2020**, 63, 2397–2428.
4. Z. Huang, H. Liu, R. Hu, H. Qiao, H. Wang, Y. Liu, X. Qi, H. Zhang. Structures, properties and application of 2D monoelemental materials (Xenes) as graphene analogues under defect engineering. *Nano Today* **2020**, 35, 100906.
5. J. Li, C. Wan, C. Wang, H. Zhang, X. Chen. 2D Material Chemistry: Graphdiyne-based Biochemical Sensing. *Chem. Res. Chin. Univ.* **2020**, 36, 622–630.
6. S.M. Beladi-Mousavi, A.M. Pourrahimi, Z. Sofer, M. Pumera. Atomically Thin 2D-Arsenene by Liquid-Phased Exfoliation: Toward Selective Vapor Sensing. *Adv. Funct. Mater.* **2018**, 1807004.
7. Z.-H. Qi, Y. Hu, Z. Jin, J. Ma. Tuning the liquid-phase exfoliation of arsenic nanosheets by interaction with various solvents. *Phys. Chem. Chem. Phys.* **2019**, 21, 12087–12090.
8. X. Wu, X. Zhang, X. Wang, Z. Zeng. Spin density waves predicted in zigzag puckered phosphorene, arsenene and antimonene nanoribbons. *AIP Advances* **2016**, 6, 045318.
9. Y.R. Wang, Z.Y. Zhang, H.N. Cao, D. Wang, Y.H. Wang, M.S. Si. Indirect-direct band gap transition in puckered arsenene through chemical doping of P, Sb and Bi: a computational study. *Materials Technology*. **2016**, 31, 4–6.
10. K.-W. Yang, M.-J. Li, X.-J. Zhang, X.-M. Li, Y.-L. Gao, M.-Q. Long. Spin-dependent transport characteristics of nanostructures based on armchair arsenene nanoribbons. *Chinese Phys. B.* **2017**, 26, 098509.
11. C. Xu, M. Zhu, H. Zheng, X. Du, W. Wang, Y. Yan. Stability, electronic structure and magnetic properties of vacancy and nonmetallic atom-doped buckled arsenene: first-principles study. *RSC Adv.* **2016**, 6, 43794–43801.
12. D. Kecik, E. Durgun, S. Ciraci. Optical properties of single-layer and bilayer arsenene phases. *Phys. Rev. B.* **2016**, 94, 205410.
13. https://pubchem.ncbi.nlm.nih.gov/compound/Benzene
14. https://pubchem.ncbi.nlm.nih.gov/compound/Phenol
15. E. Comini. Metal oxides nanowires chemical/gas sensors: recent advances. *Materials Today Advances* **2020**, 7, 100099.
16. F.K. Algethami, H.M. Marwani, A.M. Asiri, M.M. Rahman. Comparative performances of phenolic sensors based on various CeO2-carbon material nanocomposites for environmental safety. *SR.* **2018**, 38, 467–477.
17. S. Smidstrup, T. Markussen, P. Vancraeyveld et.al. QuantumATK: an integrated platform of electronic and atomic-scale modelling tools. *J. Phys.: Condens. Matter*. **2019**, 32, 015901
18. J.P. Perdew, K. Burke, M. Ernzerhof. Generalized Gradient Approximation Made Simple. *Phys. Rev. Lett.* **1996**, 77, 3865–3868.
19. J.P. Perdew, K. Burke, Y. Wang. Generalized gradient approximation for the exchange-correlation hole of a many-electron system. *Phys. Rev. B.* **1996**, 54, 16533–16539.
20. S. Grimme, J. Antony, S. Ehrlich, H. Krieg. A consistent and accurate ab initio parametrization of density functional dispersion correction (DFT-D) for the 94 elements H-Pu. *J. Chemical Physics* **2010**, 132, 154104.
21. V. Nagarajan, R. Chandiramouli. Sorption studies and removal of chlortetracycline and oxytetracycline using theta phosphorene nanoribbon – A DFT outlook. *J. Molecular Liquids* **2021**, 117070.
22. M.S. Jyothi, V. Nagarajan, R. Chandiramouli. Interaction studies of benzene and phenol on novel 4–8 arsenene nanotubes – A DFT insight. *Computational and Theoretical Chemistry* **2021**, 1204, 113381.
23. P. Jamdagni, A. Thakur, A. Kumar, P.K. Ahluwalia, R. Pandey. Two dimensional allotropes of arsenene with a wide range of high and anisotropic carrier mobility. *Phys. Chem. Chem. Phys.* **2018**, 20, 29939–29950.
24. V. Nagarajan, N. Srividya, R. Chandiramouli. Interaction studies of liver cancer biomarkers on black phosphorene sheets – A DFT outlook. *FlatChem.* **2021**, 30, 100293.
25. V. Nagarajan, S. Sundar, R. Chandiramouli. Interaction studies of tuberculosis biomarker vapours on novel beta arsenene sheets – A DFT insight. *Computational and Theoretical Chemistry* **2021**, 1205, 113426.
26. T. Jadoon, A. Ahsin, F. Ullah, T. Mahmood, K. Ayub. Adsorption mechanism of p- aminophenol over silver-graphene composite: A first principles study. *Journal of Molecular Liquids* **2021**, 341, 117415.
27. V. Nagarajan, R. Chandiramouli. Molecular adsorption studies of formaldehyde and methanol on novel twisted bilayer beta phosphorene sheets – a first-principles investigation. *Molecular Physics* **2021**, e1966535.
28. H. Sajid, F. Ullah, K. Ayub, T. Mahmood. Cyclic versus straight chain oligofuran as sensor: A detailed DFT study. *Journal of Molecular Graphics and Modelling* **2020**, 97, 107569.
29. R. Bhuvaneswari, V. Nagarajan, R. Chandiramouli. First-principles research on adsorption properties of o-xylene and styrene on 5–8 phosphorene sheets. *Chemical Physics Letters* **2021**, 765, 138244.
30. H. Sajid, K. Ayub, M. Arshad, T. Mahmood. Highly selective acridinium based cyanine dyes for the detection of DNA base pairs (adenine, cytosine, guanine and thymine). *Computational and Theoretical Chemistry* **2019**, 1163, 112509.
31. T.P. Kaloni. Tuning the Structural, Electronic, and Magnetic Properties of Germanene by the Adsorption of 3d Transition Metal Atoms. *J. Phys. Chem. C.* **2014**, 118, 25200–25208.
32. M. Sherafati, A. Shokuhi Rad, M. Ardjmand, A. Heydarinasab, M. Peyravi, M. Mirzaei. Beryllium oxide (BeO) nanotube provides excellent surface towards adenine adsorption: A dispersion-corrected DFT study in gas and water phases. *Current Applied Physics* **2018**, 18, 1059–1065.

33. A.S. Rad, E. Abedini. Chemisorption of NO on Pt-decorated graphene as modified nanostructure media: A first principles study. *Applied Surface Science* **2016**, 360, 1041–1046.
34. A. Shokuhi Rad, D. Zareyee, V. Pouralijan Foukolaei, B. Kamyab Moghadas, M. Peyravi. Study on the electronic structure of $Al_{12}N_{12}$ and $Al_{12}P_{12}$ fullerene-like nano-clusters upon adsorption of CH_3F and CH_3Cl. *Molecular Physics* **2016**, 114, 3143–3149.
35. J. Princy Maria, V. Nagarajan, R. Chandiramouli. First-principles studies on sensing properties of delta arsenene nanoribbons towards hexane and heptane molecules. *Computational and Theoretical Chemistry* **2021**, 1201, 113256.
36. M. Ghashghaee, Z. Azizi, M. Ghambarian. Theoretical insights into hydrogen sensing capabilities of black phosphorene modified through ZnO doping and decoration. *International Journal of Hydrogen Energy* **2020**, 45, 16918–16928.
37. M. Ghadiri, M. Ghashghaee, M. Ghambarian. Defective phosphorene for highly efficient formaldehyde detection: Periodic density functional calculations. *Physics Letters A* **2020**, 384, 126792.
38. A.D.O. Muñoz, A. Escobedo-Morales, E. Skakerzadeh, E.C. Anota. Effect of homonuclear boron bonds in the adsorption of DNA nucleobases on boron nitride nanosheets. *J. Molecular Liquids* **2011**, 322, 114951.
39. H. Parsa, E. Shakerzadeh, E.C. Anota. Ngn (Ng= Ne, Ar, Kr, Xe, and Rn; n=1, 2) encapsulated porphyrin-like porous $C_{24}N_{24}$ fullerene: A quantum chemical study. *J. Molecular Graphics and Modelling* **2021**, 108, 107986.
40. M.S. Jyothi, V. Nagarajan, R. Chandiramouli. Interaction studies of dichlobenil and isoproturon on square-octagon phosphorene nanotube based on DFT frame work. *Chemical Physics Letters* **2021**, 778, 138773.
41. D. Cortés-Arriagada, D.E. Ortega. Fullerene–phosphorene–nanoflake nanostructures: Modulation of their interaction mechanisms and electronic properties through the size of carbon fullerenes. *Carbon* **2021**, 182, 354–365.
42. A.A. Peyghan, M. Noei, S. Yourdkhani. Al-doped graphene-like BN nanosheet as a sensor for para-nitrophenol: DFT study. *Superlattices and Microstructures* **2013**, 59, 115–122.
43. A.A. Peyghan, H. Soleymanabadi. Adsorption of H_2S at Stone–Wales defects of graphene-like BC_3: a computational study. *Molecular Physics* **2014**, 112, 2737–2745.
44. V. Nagarajan, R. Chandiramouli. Twisted bilayer arsenene sheets as a chemical sensor for toluene and M-xylene vapours – A DFT investigation. *Journal of Molecular Graphics and Modelling* **2021**, 109, 108034.
45. A. Ahmadi Peyghan, N.L. Hadipour, Z. Bagheri. Effects of Al Doping and Double-Antisite Defect on the Adsorption of HCN on a BC2N Nanotube: Density Functional Theory Studies. *J. Phys. Chem. C* **2013**, 117, 2427–2432.
46. H. Cui, X. Zhang, Y. Li, D. Chen, Y. Zhang. First-principles insight into Ni-doped InN monolayer as a noxious gases scavenger. *Applied Surface Science* **2019**, 494, 859–866.
47. V. Nagarajan, R. Chandiramouli. Chlorobenzene and 1, 4-dichlorobenzene adsorption studies on θ-Arsenene nanosheet – a first-principles analysis. *Molecular Physics* **2021**, 119, e1936248.
48. H. Cui, X. Zhang, D. Chen, J. Tang. Pt & Pd decorated CNT as a workable media for SOF_2 sensing: A DFT study. *Applied Surface Science* **2019**, 471, 335–341.
49. H. Cui, X. Zhang, D. Chen, J. Tang. Adsorption mechanism of SF_6 decomposed species on pyridine-like PtN_3 embedded CNT: A DFT study. *Applied Surface Science* **2018**, 447, 594–598.
50. V. Nagarajan, R. Chandiramouli. ϕ-Phosphorene sheets as adsorbing medium for dichloromethane and tetrachloroethylene molecules – a DFT outlook. *Mol. Physics* **2021**, 1986163.
51. D. Ma, W. Ju, T. Li, G. Yang, C. He, B. Ma, Y. Tang, Z. Lu, Z. Yang. Formaldehyde molecule adsorption on the doped monolayer MoS2: A first-principles study. *Applied Surface Science* **2016**, 371, 180–188.
52. M.S. Jyothi, V. Nagarajan, R. Chandiramouli. Adsorption behaviour of sulfisoxazole molecules on tricycle arsenene nanoribbon - a first-principles study. *J. Mol. Liquids* **2021**, 343, 117635.
53. W. Ju, T. Li, Q. Zhou, H. Li, X. Li, D. Ma. Adsorption of 3d transition-metal atom on InSe monolayer: A first-principles study. *Computational Mater. Sci.* **2018**, 150, 33–41.
54. D. Ma, W. Ju, T. Li, X. Zhang, C. He, B. Ma, Z. Lu, Z. Yang. The adsorption of CO and NO on the MoS2 monolayer doped with Au, Pt, Pd, or Ni: A first-principles study. *Applied Surface Science* **2016**, 383, 98–105.
55. M. Yoosefian, N. Etminan. Leucine/Pd-loaded (5,5) single-walled carbon nanotube matrix as a novel nanobiosensors for in silico detection of protein. *Amino Acids* **2018**, 50, 653–661.